Annals of Nuclear Medicine (2018) 32:54–59
https://doi.org/10.1007/s12149-017-1219-7

ORIGINAL ARTICLE

Molecular imaging in musculoskeletal infections with ^{99m}Tc-UBI 29-41 SPECT/CT

Mike Sathekge[1] · Osvaldo Garcia-Perez[2] · Diana Paez[3] · Noura El-Haj[3] · Taylor Kain-Godoy[3] · Ismaheel Lawal[1] · Enrique Estrada-Lobato[3]

Received: 14 November 2017 / Accepted: 16 November 2017 / Published online: 21 November 2017

Abstract

Objective To determine the added value of CT over planar and SPECT-only imaging in the diagnosis of musculoskeletal infection using ^{99m}Tc-UBI 29-4.

Materials and methods 184 patients with suspected musculoskeletal infection who underwent planar and SPECT/CT imaging with ^{99m}Tc-UBI 29-41 were included. Planar, SPECT-only and SPECT/CT images were reviewed by two independent analysts for presence of bone or soft tissue infection. Final diagnosis was confirmed with tissue cultures, surgery/histology or clinical follow-up.

Results ^{99m}Tc-UBI 29-41 was true positive in 105/184 patients and true negative in 65/184 patients. When differentiating between soft tissue and bone infection, planar + SPECT-only imaging had a sensitivity, specificity, positive predictive value, negative predictive value and accuracy of 95.0, 74.3, 84.8, 91.3 and 86.9%, respectively, versus 99.0, 94.5, 92.5, 98.5 and 94.5% for SPECT/CT. SPECT/CT resulted in a change in reviewers' confidence in the final diagnosis in 91/184 patients. Inter-observer agreement was better with SPECT/CT compared with planar + SPECT imaging (kappa 0.87, 95% CI 0.71–0.85 versus kappa 0.81, 95% CI 0.58–0.75).

Conclusion Addition of CT to planar and SPECT-only imaging led to an increase in diagnostic performance and an improvement in reviewers' confidence and inter-observer agreement in differentiating bone from soft tissue infection.

Keywords ^{99m}Tc-UBI 29-41 · SPECT/CT · Infection · Musculoskeletal

Introduction

The diagnosis and localization of musculoskeletal infection remains a challenge for physicians as infectious diseases can be difficult to detect [1]. Molecular imaging now plays a critical role in the diagnosis of musculoskeletal infections. Radiolabelled leukocyte or white blood cell (WBC) imaging is a common modality for infection diagnosis. Its excellent diagnostic performance has led to it being considered as the gold-standard imaging modality for peripheral bone osteomyelitis. However, the process of using radiolabelled WBCs has also had a fair number of drawbacks [2]. These include the need to collect and label individual patient's blood followed by reinjection, the need for a team of well-trained staff to perform in vitro labelling as well as sufficient facilities, the risk of acquiring an infection and/or cross-contaminating samples, and the cost required for cell labelling. In response to these challenges, significant steps have been taken over the past decade in identifying and developing a suitable replacement for WBCs. Advances with antimicrobial peptides have shown promising developments, the most promising being ubiquicidin (UBI), a cationic, synthetic antimicrobial peptide fragment. Labelled with ^{99m}Tc, ^{99m}Tc-UBI 29-41 has shown a high labelling yield (> 90%) and proven stability, along with an increased biological and pharmacological performance, making it a credible candidate for infection imaging [1].

Many studies have reported on the use of planar imaging alone [1]. Lack of anatomic correlation may hamper

✉ Mike Sathekge
mike.sathekge@up.ac.za

1 Department of Nuclear Medicine, University of Pretoria and Steve Biko Academic Hospital, Private Bag X169, Pretoria 0001, South Africa

2 Nuclear Medicine Department, National Cancer Institute in México, Mexico City, Mexico

3 International Atomic Energy Agency, Vienna, Austria

delineation of bone infection from adjacent soft tissue infection. Single-photon emission computed tomography (SPECT) has better sensitivity compared to planar images due to enhanced image contrast. Addition of complementary CT imaging in the form of SPECT/CT has been shown to improve diagnostic accuracy and interpreters' confidence [3, 4]. CT provides anatomic correlation for the metabolic imaging allowing clear delineation between contiguous structures. The aim of this study was, therefore, to assess the added value of CT over planar and SPECT-only in radionuclide imaging of musculoskeletal infection with ^{99m}Tc-UBI 29-41.

Materials and methods

Patient population

One hundred and eighty-four patients (101 women and 83 men; age range 23–85 years; mean age 52.7 years) with suspected bone and soft tissue infections were enrolled. All patients exhibited clinical signs of infection (i.e. swelling, pain, heat, erythema, fever) and abnormal laboratory test results (increased white blood cell count, percentage of neutrophils, erythrocyte sedimentation rate). No patient was on antibiotic therapy prior to scintigraphy. All patients provided a written informed consent prior to enrollment. The demographic and clinical characteristics of the patients are summarized in Table 1. This retrospective study was approved by the institution's ethics committee and has been performed in accordance with the ethical standards laid down in the 1964 Declaration of Helsinki and all subsequent revisions.

Table 1 Patient characteristics ($n = 184$)

Characteristics	Number of patients/average
Sex	
Male	101
Female	83
Bloods	
Erythrocyte sedimentation rate	36 ± 15 mm/hr
C-reactive protein	104.8 mg/dL ± 35
Leukocytosis	9. 0 ± 8.2
Tissue culture	
Positive	104
Negative	17
Histology/surgery	
Positive	15
Negative	2
Clinical follow-up	46

Synthesis of ^{99m}Tc-UBI 29-41

^{99m}Tc-UBI 29-41 was prepared according to the recommendations of the IAEA publication on the reconstitution of cold kits supplied by the National Institute of Nuclear Research. These steps are as described by Sepúlveda-Méndez et al. [5]. Briefly, Tc-99m sodium pertechnetate (370 MBq in 0.5 ml 0.9% saline) was added to a vial containing 25 mg UBI (29-41) peptide, 10 µl 0.01 M acetic acid, stannous ions, and 20 µl sodium borohydrate (8.0 µl, 0.7 mg/ml in 0.1 N NaOH). The solution was allowed to stand at room temperature for 30 min. Quality control of each synthesis was done using instant thin-layer chromatography (ITLC).

Image acquisition

Whole-body and static images were obtained 30 min after injection of 555–725 MBq of ^{99m}Tc-UBI 29-41. SPECT/CT images were obtained over the region of interest 60 min post-tracer injection.

SPECT imaging was performed using a Symbia T6 gamma camera (Siemens Medical Solutions, Hoffman Estates, Illinois) equipped with low-energy and ultrahigh-resolution collimator. The energy peak was centred at 140 keV with a window of 15% and the use of non-circular orbit. Zoom was 1×, 128 steps 30 s each and a matrix size of 128 × 128 pixels. Image reconstruction was done with ordered subset expectation maximization (OSEM) iterative reconstruction (4 iterations and 8 subsets). The CT study was performed using a Siemens Sensation 6-detector (Siemens Medical Solutions, Hoffman Estates, Illinois) with a kilovoltage of 140 keV and 100 mA/s, speed of 0.6 s, collimation of 0.75 mm and reconstruction Kernel filter B2f images using filtered back-projection to produce cross-sectional images covering the same area of the SPECT study.

Both CT attenuation-corrected and non-corrected SPECT images were sent in DICOM format (Digital Imaging and Communication in Medicine) to a Siemens multi-modality workstation to be reconstructed and fused using the Syngo MI software (Siemens Medical Solutions, Hoffman Estates, Illinois). Images were evaluated in the coronal, transaxial, and sagittal planes and in tridimensional maximum-intensity-projection cine mode by the application Syngo TrueD (Siemens Medical Solutions, Hoffman Estates, Illinois) (Fig. 1b).

Image analysis and interpretation

Two experienced nuclear medicine physicians unaware of the patients' clinical history and results of prior conventional imaging independently reviewed the planar scans and SPECT/CT images with regard to the presence and

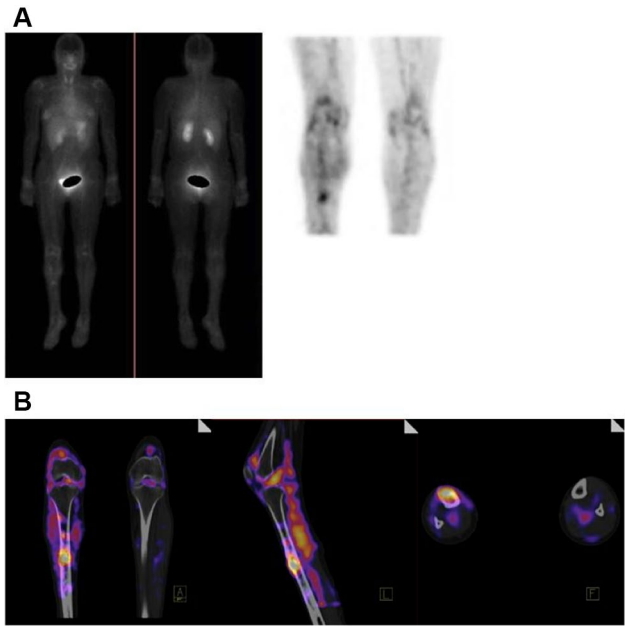

Fig. 1 ^{99m}Tc-UBI 29-41 scintigraphy of a 45-year-old man with an exposed fracture in the right leg due to an automotive vehicle accident. **a** Planar anterior (left) and posterior (right) images; can see faint ill-defined uptake of ^{99m}Tc-UBI 29-41 around the right knee and tibia. **b** SPECT/CT maximum-intensity-projection images from left to right: transaxial, sagittal, and coronal. Precise anatomic location and extent of the infection with regard to bone and soft tissue involvement of the knee and tibia is shown. There was evidence of an infection with positive culture for *Pseudomonas aeruginosa* and *Staphylococcus aureus*

location of any focus of abnormal accumulation indicating infection. Preliminary analysis of the SPECT/CT images included visual inspection to exclude misregistration between the SPECT and the CT components.

On the images, anatomically adjusted regions of interest were drawn over the entire focus of infection (target [T]) and contralateral (non-target [NT]) area. Accumulation of the tracer at sites of infection was expressed as a ratio of number of counts in the target and non-target areas (T/NT).

The images were classified as negative when no sites of abnormal uptake were observed and positive when at least one focus of abnormal uptake was characterized by a radioactivity level equal to or above that of the liver. Focal uptake indicating infection was further classified depending on presence at single or multiple sites.

Semi-quantification of the added value of SPECT/CT versus SPECT-only was measured using the method described by Roach et al. [6]. For each abnormality seen on SPECT or planar imaging, the confidence of the reviewers for both location and diagnosis was rated using the following five-point scale: (1 = little confidence, 2 = some confidence, 3 = moderate confidence, 4 = good confidence, 5 = high confidence).

Both physicians then reviewed each case concurrently and a consensus was reached in the event of disagreement. The SPECT/CT-fused images were reviewed at the workstation and the same assessment of lesion location and diagnosis was made. The confidence for both location and diagnosis was recorded using the same five-point scale as previously stated. When determining whether there was more information provided by SPECT/CT versus SPECT-only, a change in confidence of at least two points on the five-point scale was required to imply significance.

When determining whether the SPECT/CT had resulted in a change in reviewers' confidence in the final diagnosis and scan interpretation, a three-point scale was used with 0 indicating no change, 1 indicating a minor change, and 2 indicating a major change.

Data analysis and statistics

The results of ^{99m}Tc-UBI 29-41 scintigraphy were verified for each suspected site with tissue cultures (121 patients), surgery plus histology (17 patients) or by clinical follow-up of up to 6 months (46 patients) with an additional clinical follow-up of up to 12 months.

Initially, SPECT and planar images were separately assessed by the two nuclear medicine physicians unaware of the results of any prior tissue culture and radiologic investigations (CT or MRI). Hybrid imaging was subsequently evaluated, and the SPECT/CT findings were compared against findings obtained with planar and SPECT-only imaging. SPECT/CT was considered contributory if it accurately localized the anatomic site of infection and, in particular, if it discriminated between bone and soft tissue involvement. The inter-observer agreement levels were assessed with a kappa coefficient.

All values were expressed as median and range, as customary for nonparametric data. Sensitivity and specificity of ^{99m}Tc-UBI 29-41 planar, SPECT-only, and SPECT/CT imaging were calculated based on the final diagnosis.

Results

The radiochemical purity was greater than 95% in all syntheses. No additional purification was necessary after kit preparation. No adverse reaction was observed following ^{99m}Tc-UBI 29-41 administration to patients.

^{99m}Tc-UBI 29-41 scintigraphy was true positive for infection in 105 out of 184 patients and true negative in 65 out of 184 subjects. When differentiating between soft tissue versus bone infection, combined planar and SPECT imaging had a sensitivity of 95.0%, a specificity of 74.3%,

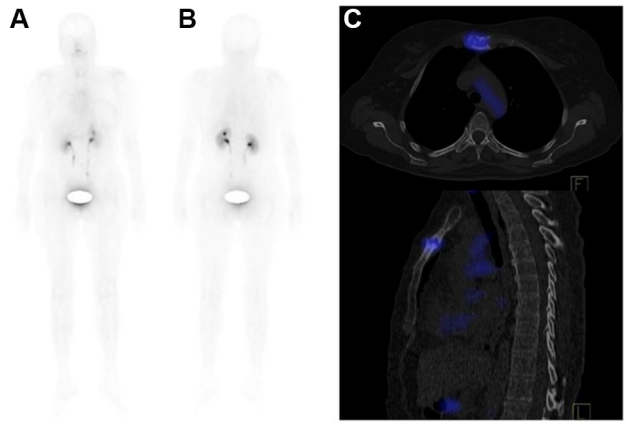

Fig. 2 SPECT/CT using ^{99m}Tc-UBI 29-41 for a 39-year-old woman with chronic myelogenous leukaemia (CML) and possible manubriosternal septic arthritis. **a** Planar images. Note: no confident diagnosis of abnormal uptake on planar images. **b** Transaxial SPECT/CT image and **c** sagittal SPECT/CT image clearly shows the abnormal focal uptake in the manubrio-sternal joint. The culture was positive for *Staphylococcus aureus*

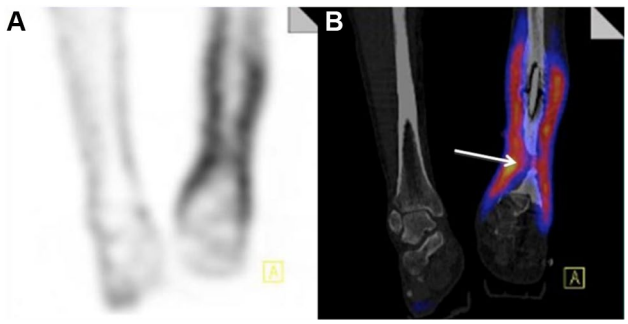

Fig. 3 ^{99m}Tc-UBI 29-41 scintigraphy of a 38-year-old man in whom posttraumatic osteomyelitis of the right tibia was suspected. **a** SPECT images show linear diffuse area of ^{99m}Tc-UBI 29-41 uptake around the intramedullary nail in the adjacent soft tissue. It is difficult to differentiate between soft tissue uptake and bone uptake. **b** SPECT/CT precisely localizes the uptake in the soft tissue and bone. Final diagnosis (made by culture) was posttraumatic tibial osteomyelitis positive for *S. epidermidis* and *Enterobacter cloacae*

a positive predictive value of 84.6%, a negative predictive value of 91.3%, and an accuracy of 86.9% (Figs. 2a, 3a). SPECT/CT, on the other hand, had a sensitivity of 99.0%, a specificity of 94.5%, a positive predictive value of 92.5%, a negative predictive value of 98.5%, and an accuracy of 94.5% (Figs. 2b, c; 3B).

Target to non-target area ratios (T/NT) were calculated at 60 min post-injection, analysed by ROC curves with a cut-off measure of 2.55 ± 0.7, a sensitivity of 100% (95% CI 63–100%), and a specificity of 97.8% (95% CI 82.47–99.94%) to differentiate between infection and non-infected areas. Furthermore, the inter-observer agreement level was higher for SPECT/CT (kappa 0.87, 95% CI 0.71–0.85) than for SPECT-only (kappa 0.81, 95% CI 0.58–0.75).

SPECT/CT contribution to final diagnosis

The interpretation of conventional scintigraphy (planar + SPECT) was changed on the basis of SPECT/CT in 91 of the 184 patients (49.4%). This change in interpretation was minor in 11.4% of patients and major in 38% of patients (Table 2). Osteomyelitis was excluded in 36 patients and the extent of infection was more accurately assessed in 27 patients.

Microorganisms

Of the microorganisms identified, Staphylococcal species were most frequently responsible for infections ($n = 47/109$), followed by *Pseudomonas aeruginosa* ($n = 18/109$), *Escherichia coli* ($n = 18/109$), and ($n = 16/109$) for *Enterococcus fecalis*. There were 13 patients with polymicrobial infection.

Discussion

In this study, we report on the added value of complementary CT imaging to planar and SPECT-only imaging of musculoskeletal infection using ^{99m}Tc-UBI 29-41. To our knowledge, this is one of the largest studies that have described this imaging modality in musculoskeletal infection and the first to have reported on the added value of complementary morphologic imaging with CT. UBI 29-41, as a cationic human antimicrobial peptide, has a high sensitivity and specificity for the detection of bacterial and fungal infections in both human and animals, including immunocompromised animals [7–9]. The Coordinated Research Project (CRP) established by the IAEA over the past decade has encouraged the evaluation of UBI as an effective tracer. Studies under the CRP and others have reported UBI to exhibit a high labelling efficiency > 90%, good stability, rapid uptake and clearance via the kidneys, excellent ability to detect infection focus and its differentiation from sterile inflammation as well as therapy response assessment [8–23].

Table 2 Additional information provided by SPECT/CT

Indication	Number of patients	No change	Minor change	Significant change
Osteomyelitis	167	96	12	59
Orthopaedic implant	17	3	3	11
Total	184	65	21	70

Detection of osteomyelitis on ^{99m}Tc-UBI 29-41 planar scans alone without anatomic landmarks may be difficult. The accuracy of imaging may be compromised when attempting to differentiate between bone and soft tissue infection as ^{99m}Tc-UBI 29-41 accumulates in soft tissue infection as well (Fig. 1a) [24].

We clearly demonstrate better accuracy with SPECT/CT imaging compared to planar and SPECT-only imaging, 94.5 versus 86.9%. The better accuracy of SPECT/CT imaging lies in its higher specificity compared to planar and SPECT-only imaging, 94.5 versus 74.3%. Both imaging techniques show satisfactory sensitivity of 95.0% for planar and SPECT-only imaging and 99.0% for SPECT/CT imaging. Sepúlveda-Méndez et al. evaluated the role of ^{99m}Tc-UBI 29-41 scintigraphy in identifying focus of infection in patients with fever of unknown origin [5]. They reported a sensitivity of 97.52%, a specificity of 95.35%, and an accuracy of 96.62%. Another study explored the use of ^{99m}Tc-UBI 29-41 scintigraphy in diabetic foot infections and reported perfect sensitivity, specificity and accuracy values of 100% [13]. Inclusion of bone scan for anatomic correlation to differentiate bone infection from infection limited to the soft tissue in the latter study is probably responsible for this excellent diagnostic performance.

A more recent study which also used ^{99m}Tc-MDP bone scan to correlate findings on ^{99m}Tc-UBI planar imaging reported sensitivity, specificity, PPV and NPV of 100, 85.7, 93.75, 100%, respectively, in 22 patients with painful prostheses evaluated for septic loosening [25]. The perfect NPV reported in this study may be attributed to the inclusion of bone scan in image interpretation. While bone scan has poor specificity for the detection of infection in a violated bone, it has an excellent negative predictive value. The inclusion of ^{99m}Tc-MDP bone scan in some of these studies emphasizes the need for some anatomic correlation.

The independent reviews conducted by two nuclear medicine physicians reported a significant increase in confidence in regard to final diagnosis and localization of infection. After an initial evaluation of the planar and SPECT-only imaging, subsequent review of the SPECT/CT imaging resulted in a change in reviewers' confidence in diagnosing the presence of infection and differentiating between bone and soft tissue infection in 49.4% of patients. The change in confidence was major in 38% of patients. Complementary anatomic CT imaging is important in delineating osteomyelitis from infection in adjacent soft tissue. This differentiation has management implication as both types of infection may be treated differently. Roach et al. evaluated the impact of inclusion of CT for anatomic correlation in a diverse type of radionuclide imaging and reported an overall change in reviewers' confidence with regard to lesion localization and in the final diagnosis in 56% of patients on the basis of inclusion of CT information [6].

Addition of CT data in image interpretation led to improvement in inter-observer agreement in differentiating soft tissue from bone infection; SPECT/CT kappa 0.87, 95% CI 0.71–0.85 and planar, and SPECT-only imaging kappa 0.81, 95% CI 0.58–0.75.

Positron emission tomographic (PET) imaging has better resolution than the SPECT system. The PET systems are now mostly hybrid in the form of PET/CT and more recently PET/MR. The better resolution of the PET camera and complementary anatomic information available from CT has led to interest in ^{68}Ga-labelled UBI 29-41 for PET imaging of infection [26]. The added value of SPECT/CT and PET/CT for diagnosing infections may ultimately increase the usefulness and accuracy of the highly specific UBI tracer by increasing its ability to provide precise anatomical locations as well as improve spatial resolution.

In an effort to improve target/non-target ratios (T/NT), a critical step during the molecular imaging process is determining at what time scans should be taken. There is a great diversity in the imaging time as reported in different studies [1]. In our study, we obtained the planar images at 30 min and the SPECT/CT images 60 min post-tracer injection. In ROC analysis, we obtained a T/NT cut-off ratio of 2.55 ± 0.7 at 60 min post-tracer injection with a sensitivity of 100% (95% CI 63–100%), and a specificity of 97.8% (95% CI 82.47–99.94%) to differentiate between infected and non-infected areas. Melendez-Alafort et al. observed a T/NT ratio of 2.18 ± 0.74 in positive lesions after 120 min and minimal accumulation in non-target tissues [7]. In a group of 50 patients with suspected musculoskeletal infection, Esmailiejah and colleagues reported a T/NT ration (lesion to background ratio) of 2.05 ± 0.41 in infection site which was significantly higher than T/NT ratio found at sites negative for infection (1.52 ± 0.22, $p < 0.001$) [27]. In their study, whole-body planar images were acquired at 60 and 120 min post-tracer injection. It is unknown on which of the two images acquired at 60 and 120 min the T/NT ratio was calculated from. This makes comparison of their T/NT ratios with those of other studies difficult. Our T/NT cut-off ratio obtained at 60 min post-tracer injection appears to have sufficient sensitivity and specificity to differentiate between infection and its absence. We, therefore, speculate that a waiting period of 60 min prior to imaging is sufficient and that it may be unnecessary to wait for 120 min post-tracer injection for image acquisition.

In conclusion, ^{99m}Tc-UBI 29-41 scintigraphy has an excellent diagnostic performance in the evaluation of musculoskeletal infection. Addition of CT morphologic imaging to planar and SPECT-only imaging led to an increased in diagnostic performance and an improvement

in diagnostic confidence in differentiating soft tissue from bone infection as well as a higher inter-observer agreement.

References

1. Ferro-Flores G, Avila-Rodriguez MA, Garcia-Perez FO. Imaging of bacteria with radiolabeled ubiquicidin by SPECT and PET techniques. Clin Transl Imaging. 2016;4:175–82.
2. Lawal I, Zeevaart JR, Ebenhan T, Ankrah A, Vorster M, Kruger HG, et al. Metabolic imaging of infection. J Nucl Med. 2017;58:1727–32.
3. Bar-Shalom R, Yefremov N, Guralnik L, Keidar Z, Engel A, Nitecki S, et al. SPECT/CT using 67 Ga and 111In-labeled leukocyte scintigraphy for diagnosis of infection. J Nucl Med. 2006;47:587–94.
4. Filippi L, Schillaci O. Usefulness of hybrid SPECT/CT in 99mTc-HMPAO-labeled leukocyte scintigraphy for bone and joint infections. J Nucl Med. 2006;47:1908–13.
5. Sepúlveda-Méndez J, de Murphy CA, Rojas-Bautista JC, Pedraza-López M. Specificity of 99mTc-UBI for detecting infection foci in patients with fever in study. Nucl Med Commun. 2010;31:889–95.
6. Roach PJ, Schembri GP, Ho Shon IA, Bailey EA, Bailey DL. SPECT/CT imaging using a spiral CT scanner for anatomical localization: impact on diagnostic accuracy and reporter confidence in clinical practice. Nucl Med Commun. 2006;27:977–87.
7. Meléndez-Alafort L, Rodrìguez-Cortés J, Ferro-Flores G, Arteaga de Murphy C, Herrera-Rodriguez R, Mitsoura E, et al. Biokinetics of 99mTc-UBI in humans. Nucl Med Biol. 2004;31:373–9.
8. Jehangir M, Bashar M, Pervez S. Development of kits for ^{99m}Tc radiopharmaceuticals for infection imaging. IAEA-TECDOC-1414. 2004;65–77.
9. Mikolajczak R, Korsak A, Gorska B, Markiewiz E, Zakrzewska W, Zulczyk U, et al. Development of kits for ^{99m}Tc radiopharmaceuticals for infection imaging. IAEA-TECDOC-1414. 2004;79–86.
10. Akhtar MS, Iqbal J, Khan MA, Irfanullah J, Jehangir M, Khan B, et al. 99mTc-labeled antimicrobial peptide ubiquicidin (29-41) accumulates less in Escherichia coli infection than in Staphylococcus aureus infection. J Nucl Med. 2004;45:849–56.
11. Nibbering PH, Welling MM, Paulusma-Annema A, Brouwer CP, Lupetti A, Pauwels EK. 99mTc-Labeled UBI 29-41 peptide for monitoring the efficacy of antibacterial agents in mice infected with Staphylococcus aureus. J Nucl Med. 2004;45:321–6.
12. Signore A, D'Alessandria C, Lazzeri E, Dierckx R. Can we produce an image of bacteria with radiopharmaceuticals? Eur J Nucl Med Mol Imaging. 2008;35:1051–5.
13. Saeed S, Zafar J, Khan B, Akhtar A, Qurieshi S, Fatima S, et al. Utility of ^{99m}Tc-labelled antimicrobial peptide ubiquicidin (29-41) in the diagnosis of diabetic foot infection. Eur J Nucl Med Mol Imaging. 2013;40:737–43.
14. Welling MM, Paulusma-Annema A, Balter HS, Pauwels EK, Nibbering PH. Technetium-99m labelled antimicrobial peptides discriminate between bacterial infections and sterile inflammations. Eur J Nucl Med. 2000;27:292–301.
15. Lupetti A, Welling MM, Pauwels EK, Nibbering PH. Radiolabelled antimicrobial peptides for infection detection. Lancet Infect Dis. 2003;3:223–9.
16. Akhtar MS, Qaisar A, Irfanullah J, Iqbal J, Khan B, Jehangir M, et al. Antimicrobial peptide 99mTc-ubiquicidin 29-41 as human infection-imaging agent: clinical trial. J Nucl Med. 2005;46:567–73.
17. Welling MM, Lupetti A, Balter HS, Lanzzeri S, Souto B, Rey AM, et al. 99mTc-labeled antimicrobial peptides for detection of bacterial and Candida albicans infections. J Nucl Med. 2001;42:788–94.
18. Arteaga de Murphy C, Gemmel F, Balter J. Clinical trial of specific imaging of infections. Nucl Med Commun. 2010;8:726–33.
19. Assadi M, Vahdat K, Nabipour I, Sehhat MR, Hadavand F, Javadi H, et al. Diagnostic value of 99mTc-ubiquicidin scintigraphy for osteomyelitis and comparisons with 99mTc-methylene diphosphonate scintigraphy and magnetic resonance imaging. Nucl Med Commun. 2011;32:716–23.
20. Akhtar MS, Khan ME, Khan B, Irfanullah J, Afzal MS, Khan MA, et al. An imaging analysis of (99 m)Tc-UBI (29-41) uptake in S. aureus infected thighs of rabbits on ciprofloxacin treatment. Eur J Nucl Med Mol Imaging. 2008;35:1056–64.
21. Crudo J, Zapata A, Nevares N, Obanaus E, Castiglia SG de. In vitro and in vivo evaluation of ^{99m}Tc-labelled peptides for infection imaging. IAEA-TECDOC-1414. 2004;11–22.
22. Widjaksana W, Yunita F, Andriastuti L, Ariyanto YA, Mondrida G, Roseliana A, et al. ^{99m}Tc labelling of ubiquicidine (UBI 29-41) and EDTA-biotin monomer (EB1). IAEA-TECDOC-1414. 2004;41–53.
23. Signore A, Glaudemans AW. The molecular imaging approach to image infections and inflammation by nuclear medicine techniques. Ann Nucl Med. 2011;25:681–700.
24. Buck AK, Nekolla S, Ziegler S, Beer A, Krause BJ, Herrmann K, et al. SPECT/CT. J Nucl Med. 2008;49:1305–19.
25. Shinto AS, Mukherjee A, Karuppusamy KK, Joseph J, Bhatt J, Korde A, et al. Clinical utility of ^{99m}Tc-Ubiquicidin (29-41) as an adjunct to bone scan in differentiating infected versus non-infected loosening of prosthesis before revision surgery. Nucl Med Commun. 2017;38:285–90.
26. Ebenhan T, Zeevaart JR, Venter JD, Govender T, Kruger GH, Jarvis NV, et al. Preclinical evaluation of 68 Ga-labeled 1,4,7triazacyclononane-1,4,7-triacetic acid-ubiquicidin as a radioligand for PET infection imaging. J Nucl Med. 2014;55:308–14.
27. Esmailiejah AK, Abbasian M, Azarsina S, Safdari F, Amoui M, Hosseinzadeh S. Diagnostic efficacy of UBI scan in Musculoskeletal infections. Arch Iran Med. 2015;18:371–5.